



Gazi University

**Journal of Science**

PART A: ENGINEERING AND INNOVATION

<http://dergipark.org.tr/guj.1514851>

## Development of a P(L-D,L)LA Foam as a Dura Substitute and Its *In Vitro* Evaluation

Deniz YÜCEL<sup>1,2\*</sup> <sup>1</sup> Acıbadem Mehmet Ali Aydınlar University (ACU), School of Medicine, Department of Histology and Embryology, İstanbul, Türkiye<sup>2</sup> Acıbadem Mehmet Ali Aydınlar University (ACU), ACU Biomaterials Center, İstanbul, Türkiye

Keywords	Abstract
Dura Substitute Synthetic Polymer Porous Foam Meningeal Cells Cell Ingrowth	Dura substitutes are used to reduce the risk of postoperative complications following neurosurgical interventions, and to facilitate the healing of dura damages or defects caused by injuries. Traditional tissue transplants have limitations like limited tissue availability, potential risk of immune rejection and disease transmission. The use of biomaterials composed of synthetic polymers as dura substitutes offers a promising approach to overcome these limitations to replace and treat damaged dura mater. Potential biocompatible porous scaffolds still need to be developed to minimize the risks of immune response and disease transmission, while also ensuring effective cell migration and cell ingrowth in three dimension. The aim of the present study was to develop a poly(L-lactide-co-D,L-lactide) (P(L-D,L)LA) foam with an optimal pore size for dura mater substitution, investigate its morphological characteristics, and evaluate its potential for dura mater regeneration by assessing the spreading and growth of meningeal cells within it through <i>in vitro</i> studies. Foams were produced by lyophilization using different concentrations of P(L-D,L)LA solution. A GMP-grade P(L-D,L)LA, suitable for medical device applications, was used in this study. Morphological analysis was performed using scanning electron microscopy, and porosity of the foams was studied with mercury porosimetry. In <i>in vitro</i> studies, meningeal cells were seeded onto the polymeric foams, and their behavior and proliferation in these scaffolds were investigated with cytoskeleton and nucleus staining, and colorimetric cell proliferation assay, respectively. Scanning electron microscopy results showed that the foams prepared with 2.5% and 3% polymer solutions displayed good structural integrity and convenient interconnectivity, with pore sizes ranging from 80 to 150 $\mu\text{m}$ . However, the foams prepared with 2% and 4% polymer solution demonstrated poor structural integrity and low interconnectivity, respectively. <i>In vitro</i> studies showed that the foams prepared with 2.5% and 3% polymer solutions served effectively as scaffolds for meningeal cells, and the cells attached, spread and homogeneously distributed. In addition, the cells proliferated and increased in number over time within these polymeric scaffolds. These findings suggest that the foams produced with 2.5% and especially 3% P(L-D,L)LA polymer solutions could effectively serve as a suitable substitute for the dura mater, providing an appropriate environment for cell ingrowth and tissue integration. This indicates that the developed foam could be a promising treatment for dura mater damage or defects, with the potential approach to promote regeneration in future <i>in vivo</i> and clinical studies.

### Cite

Yucel, D. (2024). Development of a P(L-D,L)LA Foam as a Dura Substitute and Its In Vitro Evaluation. *GU J Sci, Part A, 11(3)*, 507-517. doi:10.54287/guj.1514851

Author ID (ORCID Number)	Article Process
0000-0002-1373-5183 Deniz YÜCEL	<b>Submission Date</b> 11.07.2024 <b>Revision Date</b> 28.08.2024 <b>Accepted Date</b> 16.09.2024 <b>Published Date</b> 28.09.2024

## 1. INTRODUCTION

The meninges are connective tissue layers covering brain and spinal cord, and consist of pia, arachnoid and dura mater from the innermost to the outermost layer (Patel & Kirmi, 2009). The meninges are important in protecting the central nervous system (CNS) by serving as a structural support and facilitating the circulation of cerebrospinal fluid (CSF). The pia mater, thin and highly vascular connective tissue layer, surrounds the

\*Corresponding Author, e-mail: [deniz.yucel@acibadem.edu.tr](mailto:deniz.yucel@acibadem.edu.tr)

nervous tissue of brain and spinal cord, providing nourishment to these tissues. The arachnoid mater, comprised of a delicate sheet of connective tissue and extending trabeculae to the pia mater, forms an intricate network structure. Serving as a barrier between pia and dura maters, it establishes the subarachnoid space, housing cerebral arteries and cerebrospinal fluid (CSF). Trabeculae consist of loose connective tissue with elongated fibroblasts. The outermost layer, dura mater is a relatively thick layer of dense connective tissue continuing at the outer surface with the periosteum of the skull and provides a protective barrier against physical impacts. The dura mater contains a periosteal dura layer that attaches to the inner side of the skull and serves as the periosteum. This outer layer of dura mater consists of organized bundles of collagen fibers with fibroblasts and osteoblasts. The innermost layer, meningeal dura mater, is composed of sheet-like layers containing fine collagen fibers with fibroblasts.

After surgeries involving the brain or spinal cord, such as tumor resection, discectomy/artificial disc replacement, laminectomy, or minimally invasive surgeries, the dura mater needs to be repaired or replaced (Dong et al., 2023). In addition, there may be defects or tears in the dura mater due to injury by trauma like skull fracture and spinal burst fracture, infection, or congenital conditions. When a dural defect is too large for direct repair with suturing, the use of dura grafts to patch or close the defect through a duraplasty procedure is a potential treatment strategy to repair or reinforce the damaged dura mater and prevents CSF leakage. Dura grafts and dura substitutes serve to restore the integrity of the dura mater, to prevent complications such as infections or CSF leaks, and provide protection to the underlying neural tissues. There are traditional tissue transplants like autografts, allografts, and xenografts for the treatment of the dural defects (Khurana et al., 2024). Despite the successful results of autologous grafts with a low risk of immune rejection, they have inherent disadvantages such as limited tissue supply and donor site morbidity. Even though allografts and xenografts are available, these grafts may carry a high risk of immune rejection and a potential risk of disease transmission (Shijo et al., 2017). An alternative treatment approach is the use of biomaterials as a dura substitute to repair dural defects.

The biomaterial used as a dura substitute should be biocompatible, provide a scaffold for cell adhesion and tissue ingrowth, and promote the regeneration of dural tissue. Even though non-biodegradable materials like silicone have been used for dural repair, they are more prone to foreign-body reactions for a long time and may provoke significant complications (Ohbayashi et al., 1994). However, biodegradable dura substitutes are advantageous because they provide essential support during the healing of the dural defect, gradually dissolve and are replaced by newly formed tissue, and their complete degradation eliminates the possible risk of long-term foreign-body reaction (Wang & Ao, 2019, Cho et al., 2024). Biodegradable biomaterials can be natural polymers like collagen, or synthetic polymers like polyesters, or a combination of both (Shi et al., 2016; Deng K. et al., 2017; Deng W. et al, 2021; Liu et al., 2021). Natural polymer-based dural substitutes consist of mostly collagen (Mai et al., 2024) as well as bacterial cellulose (Deng W. et al., 2021). However, natural polymers have some drawbacks like potential risk of disease transmission associated with some animal-derived polymers, limited control over *in vivo* degradation and poor mechanical properties (Khurana et al., 2024). Synthetic polymers with their tunable properties and lack of disease transmission risk may address these issues associated with the natural polymers (Shi et al., 2016). In addition, synthetic biodegradable materials offer advantages such as being available in larger quantities, eliminating the need for a secondary surgery, allowing for the manufacturing of desired dimensions and properties, and ensuring consistent quality. Biodegradable synthetic polymers like the most commonly used polyesters poly(lactic acid) (PLA), poly(glycolic acid) (PGA), and poly( $\epsilon$ -caprolactone) (PCL) are biocompatible and tunable according to demand, which makes them preferable in medical applications (Deng K. et al., 2017). Poly-L-lactide (PLLA) has been commonly used to develop dura substitutes (Shi et al., 2016; Klopp et al., 2004; Wang Y.-f. et al., 2013; Deng K. et al., 2017). Studies have demonstrated its full compatibility with dural tissue, its integration with the surrounding tissue, its ability to reduce tissue adhesion and prevent CSF leakage (Klopp et al., 2004; Wang Y.-f. et al., 2013). Poly(L-lactide-co-D,L-lactide) (P(L-D,L)LA), a biocompatible polymer composed of poly-L-lactide and racemic DL-lactide, has been used in clinical applications in ratios of 70:30, 80:20, 85:15, and 96:4 (Schachtner et al., 2019). The commonly utilized P(L-D,L)LA (70:30) displays degradation within 1-3 years, decreasing the potential for adverse tissue reactions.

Dural substitutes can be in various forms, including film, mesh, membrane and sponge/foam, or combination of these. The film consisting of P(L-D,L)LA (70:30) polymer, with its hydrophobic nature, was used only as

a barrier to reduce the peridural tissue adhesion (Welch et al., 2002; Klopp et al., 2004). There are also electrospun fibrous meshes consisting of PLLA (Shi et al., 2016; Liao et al., 2021; Cho et al., 2024), PLLA-gelatin (Deng K. et al., 2017), and PLA-PCL-collagen (Wang Y.-f. et al., 2013) to be used for dural repair. Electrospun fibrous meshes have porosity that depends on fiber diameter and process parameters. However, due to the sheet-like assembly process of electrospinning, adequate porosity is typically achieved on the surface, while porosity in the bulk region is often limited (Guimarães et al., 2010). The tightly packed fibrous layers may restrict cell infiltration into the scaffold and inhibit the growth of 3D tissues. Porous scaffolds provide voids that facilitate the penetration of the patient's autologous cells and promote tissue renewal (Deng K. et al., 2017). The porosity within the entire scaffold is crucial, as it enables cell migration and tissue growth to ensure the degradation of the scaffold and the reformation of the dura mater. It was reported that by the fourth day after surgery, fibroblasts and histocytes started moving towards the implanted dural substitute and entered the implant through pores of the scaffold (Laun et al., 1990).

In this study, the aim was to develop a biodegradable foam with optimum pore size as a dura substitute and to assess this biomaterial's potential effectiveness in promoting dura regeneration by investigating its suitability for meningeal cell growth through *in vitro* studies. A GMP grade polymer of P(L-D,L)LA (70:30) was selected for its biocompatibility, biodegradability, and its ability to be tailored to achieve the desired scaffold morphology. In this study, foam/sponge of P(L-D,L)LA (70:30) was developed as a dura substitute to provide the necessary porosity for cell infiltration and proliferation considering the ultimate aim of enhancing the regeneration and healing process of the dura mater in the future clinical use. Dura scaffolds were produced in sponge form using different concentrations of P(L-D,L)LA. Their porous structures were shown morphologically, and pore size distribution was analyzed with mercury porosimetry. The meningeal cell integration, growth and morphology of cells in the 3D foams were demonstrated by colorimetric cell proliferation assay and Phalloidin-DAPI (2-(4-Amidinophenyl)-6-indolecarbamide) staining. This 3D porous polymeric scaffold could be a promising dura substitute to be used in the treatment of dural defects.

## 2. MATERIAL AND METHOD

### 2.1. Preparation of Polymeric Foams

#### 2.1.1. Production of Polymeric Foams

3D foams were produced using a biodegradable, synthetic polymer, P(L-D,L)LA (70:30) (GMP grade, Mw. ca. 1.500.000 g/mol, PURAC, Corbion, Netherland). The stock polymer solution (4%, w/v%) was prepared by dissolving P(L-D,L)LA in 1,4-dioxane (ACS reagent,  $\geq 99.8\%$ ) by occasionally mixing for 24 h (Kenar et al., 2010; Choi et al., 2010). Afterwards, this stock polymer solution was diluted with 1,4-dioxane to prepare 2%, 2.5% and 3% working polymer solutions. Different concentrations of P(L-D,L)LA solutions were poured into petri plates, and kept at  $-20^{\circ}\text{C}$  overnight. Frozen samples were completely dried with lyophilization, and 3D porous foams were obtained.

#### 2.1.2. Characterization of Polymeric Foams

The morphology and the porosity of the foams' surface and bulk were investigated with scanning electron microscope (SEM). The polymeric foams were coated with Au under vacuum, and then examined using SEM. In addition to surface analysis, a set of samples was cut before coating, and cross-section images were taken to assess the porosity inside the sponge. The porosity of the foams was quantitatively assessed by measuring pore area with Image J software using SEM images of three different regions. In addition, the distribution of pore sizes of the foams was analyzed using mercury porosimetry under low vacuum.

### 2.2. Culture of Meningeal Cells

Human meningeal cells (cell line, HMC, ScienCell Research Laboratories) were seeded on fibronectin ( $5\mu\text{g}/\text{cm}^2$ ) coated tissue culture plates, and cultured with a growth medium composed of  $\alpha$ -MEM: F12 (1:1) including 10% FBS and Pen/Strep (100 U/mL, 100  $\mu\text{g}/\text{mL}$ ) in an incubator (5%  $\text{CO}_2$ ,  $37^{\circ}\text{C}$ ) by refreshing medium every three days. Once the cell confluency was approximately 90%, they were detached from the tissue culture plates by treatment of trypsin/EDTA. The cells were centrifuged at 1000 rpm, and then

subcultured by transferring into new fibronectin coated tissue culture plates, and kept in the growth medium containing 10% DMSO in the vapor of liquid nitrogen until use.

### 2.3. Investigation of Meningeal Cell Behavior in the Polymeric Foams

#### 2.3.1. Seeding and Culture of Cells in the Foams

Before cell seeding, the foams prepared with two different polymer concentrations (2.5% and 3%) were kept in 70% ethanol at 4°C for 2 h for sterilization. After removing the ethanol and air drying of the foams, the foams were coated with fibronectin (50 µg/mL, 100 µL/foam) for 2h at 37°C to promote the attachment of meningeal cells. The foams were ready for cell seeding after drying slightly to a wet state. Meningeal cells were collected by trypsinization from tissue culture plates, centrifuged at 1000 rpm, and then resuspended in the growth medium. After counting with a hemocytometer, the cells at a density of  $5 \times 10^4$  cells/foam were seeded onto the foams and cultured with the growth medium in a humidified 5% CO<sub>2</sub> incubator at 37°C by refreshing medium every three days.

#### 2.3.2. Distribution and Morphology of the Meningeal Cells on/in the Foams

In order to visualize the meningeal cells in the foams, fixation of the cells on day 14 of the culture was done with 4% paraformaldehyde for 1h at room temperature (RT). The morphology of the cells was examined by staining with fluorescein isothiocyanate (FITC) conjugated Phalloidin and 2-(4-Amidinophenyl)-6-indolecarbamidine (DAPI) for cytoskeletal actin filaments and nucleus, respectively (Yucel et al., 2010). The cells were kept in 0.1% Triton X-100 solution for 5 min at RT to permeabilize cell membrane and allow dye penetration. After PBS wash, the samples were incubated in 1% bovine serum albumin (BSA) for 30 min at 37°C to prevent non-specific binding. Subsequently, the samples were incubated in FITC-Phalloidin solution (1:100 diluted with 0.1% BSA) for 1 h at 37°C. Following another wash with PBS, the nuclei of cells were stained with DAPI (1:5000, diluted with PBS) for 10 min at RT. After a final wash with PBS, the cells in the foams were examined and viewed with a Laser Scanning Confocal Microscope (LSCM, Zeiss LSM700) using 488 nm and 405 nm lasers. Optical sections were taken in z-direction, and the images were obtained using the ZenPlus program to investigate the distribution and morphology of the meningeal cells in the 3D foams.

#### 2.3.3. Proliferation of the Cells in the Foams

In order to determine the meningeal cell survival and growth in the foams, the cell-seeded foams were transferred into new 24 well plates at the 1<sup>st</sup>, 7<sup>th</sup>, 14<sup>th</sup> and 21<sup>st</sup> days of the culture, and a colorimetric cell proliferation assay (MTS) was applied to the samples which were studied in triplicates (Yucel et al., 2010). A 10% solution of MTS-PMS prepared in DMEM low glucose including 10% FBS and Pen/Strep (100 U/mL, 100 µg/mL) was added to the cell-seeded foam samples, and the cells were incubated in an incubator (5% CO<sub>2</sub>, 37°C) for 2 h. At the end of incubation, 200 µL of the reaction solution from each sample was placed into 96 well-plate, and the absorbance value was measured at 490 nm using Elisa-Plate Reader. The cell numbers were determined using the slope of the calibration graph ( $y=0.0201x$ ). The calibration graph was constructed by measuring the absorbance of known, specific cell seeding numbers with an ELISA plate reader. The slope of the graph was used to calculate the cell numbers based on the absorbance values measured from the samples.

### 2.4. Statistical Analyses

GraphPad Prism 10.0 software was used for statistical analyses. The sample data was confirmed by Shapiro-Wilk test to check if the data was normally distributed. A one-way analysis of variance (ANOVA) was used to compare mean cell numbers by day in both groups, while a two-way ANOVA was used for the comparison between groups. A minimum confidence level of 95% was set, and p-values smaller than or equal to 0.05 were considered statistically significant. All values were reported as the mean ± standard deviation.

## 3. RESULTS AND DISCUSSION

### 3.1. Morphology and Porosity Analysis of Polymeric Foams

Biomaterials should be designed to address the target tissue architecture, appropriate porosity with interconnected pores, and a tissue-specific 3D shape. Therefore, foam structures in a circular shape with a

diameter of 9 mm were constructed as a dura substitute in this study for characterization and *in vitro* studies. However, the shape and the dimensions of the foams could be altered according to the specific application. The surface and bulk morphology of the foams were examined with SEM (Figure 1). It was observed that the foams with a thickness of  $0.93 \pm 0.32$  mm, prepared using a 2% P(L-D,L)LA polymer concentration, exhibited compromised structural integrity compared to those prepared with higher polymer concentrations (Figure 1a and 1e). In addition, the pore sizes were around 300  $\mu\text{m}$ , and there was a significant variation in pore size distribution. This less robust foam network can limit its handling and performance, particularly in clinical applications that require consistent and durable materials. SEM results showed that the foams with thicknesses of  $1.74 \pm 0.11$  mm and  $1.92 \pm 0.15$  mm, produced using polymer concentrations of 2.5% and 3% P(L-D,L)LA, respectively, exhibited high structural integrity, and their pore sizes ranged between 80-150  $\mu\text{m}$  (Figure 1b and 1c, Figure 2a and 2c). In addition, it was seen in the cross-section views that this porosity continued throughout the interior of the foams, and there were interconnected pores (Figure 1f and 1g). In the foams prepared with a polymer concentration of 4% P(L-D,L)LA and a thickness of  $2.48 \pm 0.22$  mm, the structural integrity was good, and the pore sizes were in the range of 80-100  $\mu\text{m}$  (Figure 1d and 1h). However, upon examining cross-sectional images, it was noticed that some pores were closed and the interconnectivity of pores in the foam prepared with a polymer concentration of 4% was poor. Therefore, it was thought that this structure may limit the cell ingrowth and provide a less favorable environment for dura regeneration and tissue integration compared to other foams. Consequently, as expected, increasing the polymer concentration to levels such as 2.5% and 3% provided better structural integrity and led to a reduction in pore size. However, further increase in polymer concentration to 4% decreased the interconnectivity of pores. Therefore, it was decided to continue the further analysis with foams prepared with 2.5% and 3% P(L-D,L)LA solution. Using the surface and cross-section SEM images, the porosities of the foams' surface and bulk were determined by calculating the percentage of pore area (Table 1). The foams produced with polymer concentrations of 2.5% and 3% P(L-D,L)LA exhibited similar porosity levels both at the surface (ca. 58%) and in the bulk (ca. 48%). It was revealed that scaffolds with a porosity of 46.9% promoted the growth of osteocytes (Wang M. O. et al., 2015). It was also reported in the literature that fibroblast could even infiltrate scaffolds with an average porosity of 34.4% and mean pore size of 11  $\mu\text{m}$  (Rnjak-Kovacina et al., 2011). Therefore, it was thought that the porosity of the dura substitute developed in this study would provide a suitable environment for osteocyte ingrowth and the formation of the periosteal dura layer, as well as for the ingrowth of fibroblast-like meningeal cells that would regenerate the meningeal dura mater.

In Figure 2b and 2d, mercury porosimetry results show the distribution of the pore size throughout the foams produced with the polymer solutions of 2.5% and 3% P(L-D,L)LA. It was observed that the pore sizes varied in the range of 20-130  $\mu\text{m}$  and 20-200  $\mu\text{m}$  in the foams of 2.5% and 3% P(L-D,L)LA, respectively. The pore sizes ranging from 80 to 150  $\mu\text{m}$  seen in the SEM images were in the range of pore sizes determined with mercury porosimetry, thus demonstrating consistency in these results. A porous scaffold made of chitin and bacterial cellulose was developed as a dura graft with pore sizes ranging from 90 to 200  $\mu\text{m}$  and high pore connectivity, similar to the pore size range obtained in this study (Deng W. et al., 2021). In fact, the range determined in the present study is narrower, indicating that more homogeneous pore sizes were obtained. In addition, it was reported that a collagen dura substitute with interconnected pores ranging from a few micrometers to 150  $\mu\text{m}$  was suitable for cell infiltration, proliferation, and the exchange of nutrients and waste (Liu et al., 2021). It was also revealed that endogenous cells would infiltrate and proliferate within the porous scaffold and gradually reconstruct the extracellular matrix to regenerate tissue. In another study, it was observed that as the porous scaffold degraded, the newly formed tissue replaced it, ultimately leading to the repair and regeneration of the dura mater (Ramot et al., 2024).

Consequently, considering their high structural integrity, appropriate pore size, and interconnectivity, the foams produced with 2.5% and 3% P(L-D,L)LA were utilized in the further studies to investigate the behaviour of meningeal cell on these constructs.

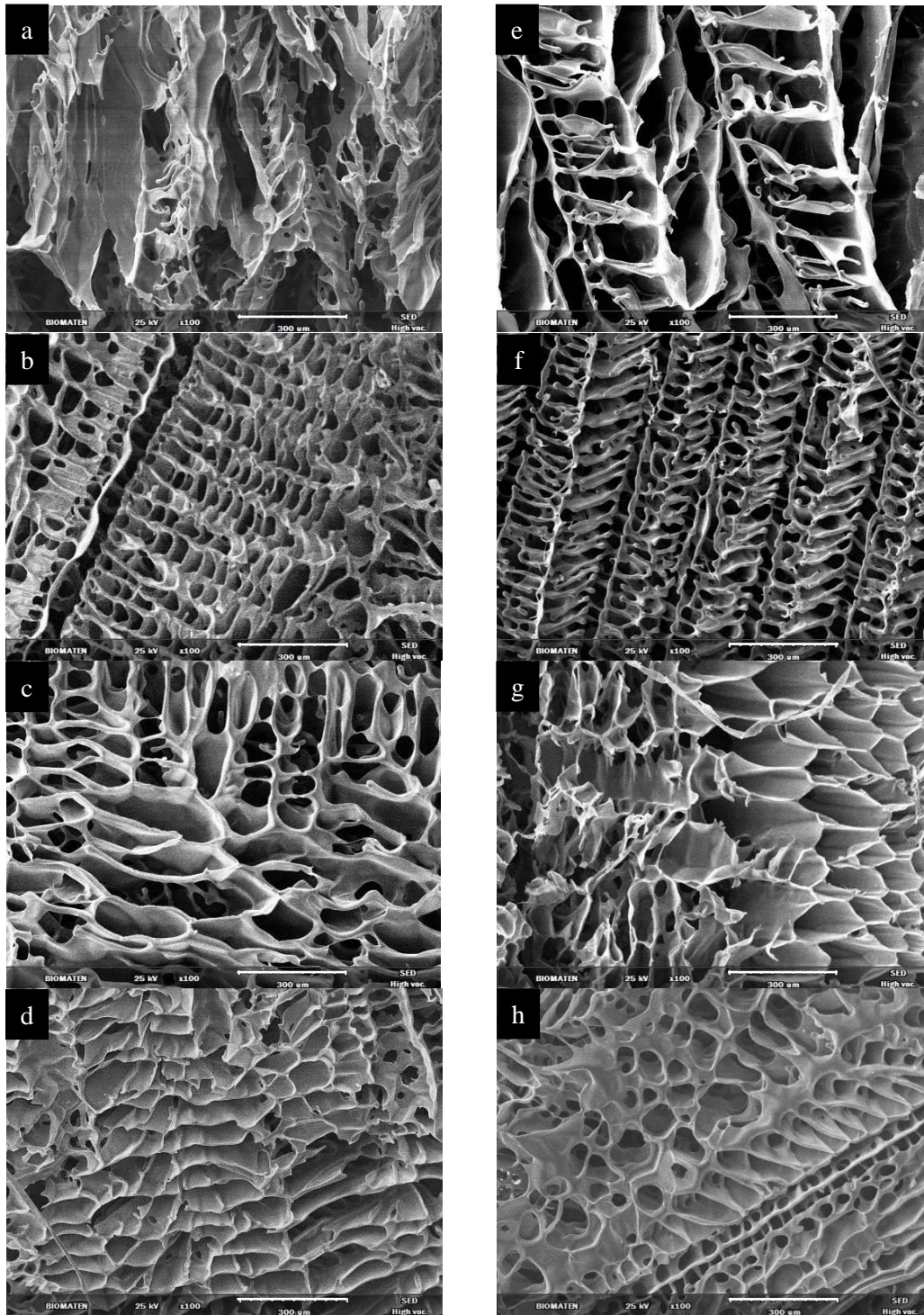


**Figure 1.** Scanning electron micrographs of the polymeric foams. The foams prepared using the polymer solutions of **a, e**) 2%, **b, f**) 2.5%, **c, g**) 3% and **d, h**) 4% P(L-D,L)LA. The images of **a-d**) the surface and **e-h**) cross-section of the foams. Magnification: 100X, scale bar: 300 $\mu$ m.

**Table 1.** Porosity analysis of the foams from the top and cross-section views.

	Foam with 2.5% P(L-D,L)LA	Foam with 3% P(L-D,L)LA
Surface	57.04 $\pm$ 0.58	58.41 $\pm$ 0.13
Cross-Section	48.16 $\pm$ 0.28	48.26 $\pm$ 1.63

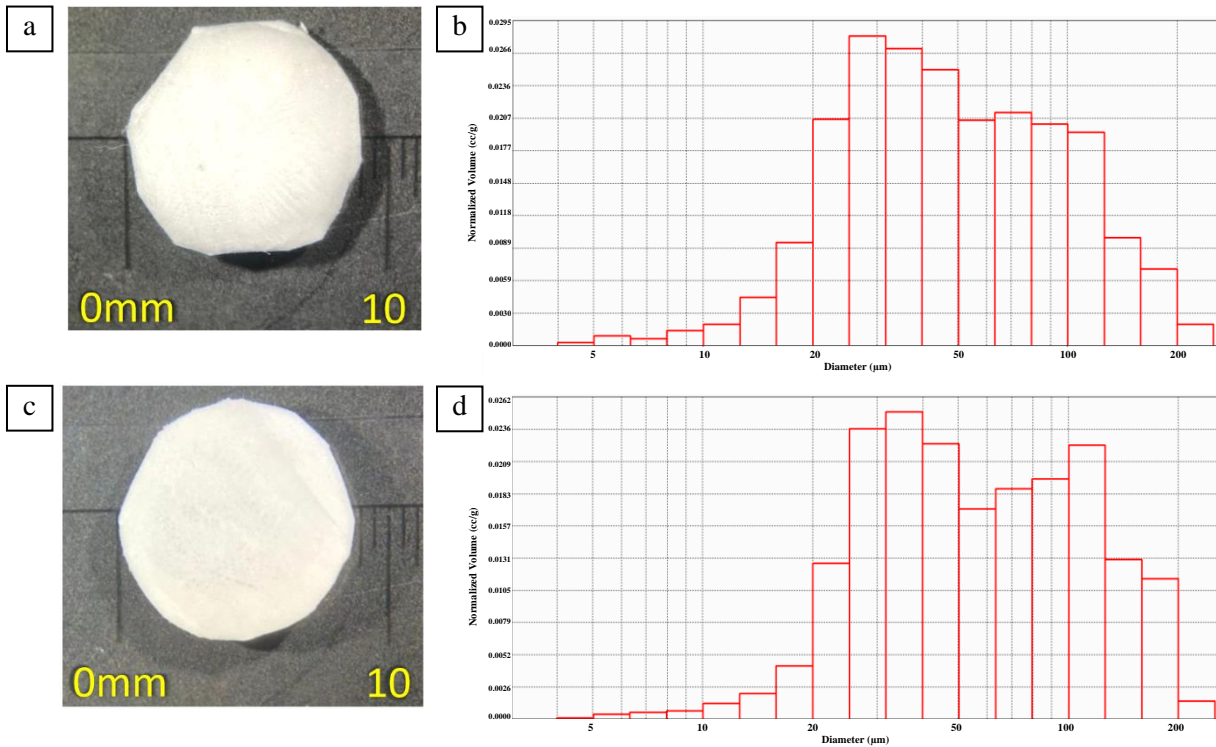


**Figure 2.** Stereomicrographs of foams prepared with **a)** 2.5% and **c)** 3% P(L-D,L)LA polymer solutions. Distribution of pore size of the polymeric foams prepared using the polymer solutions of **b)** 2.5% and **d)** 3% P(L-D,L)LA with normalized volume vs pore size histogram of the foams.

### 3.2. Culture of Meningeal Cells

Human meningeal cells cultured with the growth medium grew and increased in number on the fibronectin coated tissue culture plate (Figure 3a). Meningeal cells without any treatment could not properly adhere and spread on untreated P(L-D,L)LA due to its hydrophobic nature. Therefore, the foams were coated with fibronectin which takes role in cell adhesion, migration and growth (Mekhail et al., 2012). It was seen that the meningeal cells spread properly on the culture plate and their actin filaments were well-organized (Figure 3b). The scanning electron micrograph in Figure 3c showed the human meningeal cell interaction with the foam surface. The cells adhered well to the surface, formed filopodia, and expanded on the polymeric foam.

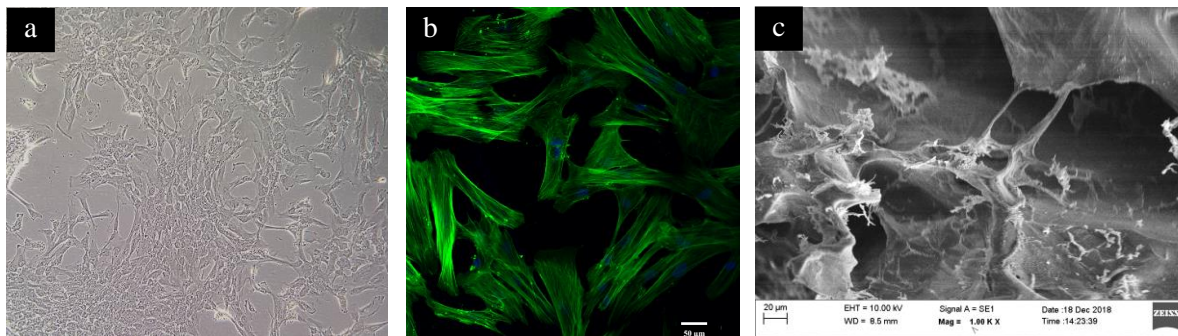


**Figure 3.** Morphology of the human meningeal cells. Images of the cells on the tissue culture plate **a)** with bright field microscope and **b)** with fluorescence microscope after Phalloidin-DAPI staining for actin filaments (green) and nucleus (blue). **c)** SEM image of the meningeal cells on the polymeric foam.

### 3.3. Meningeal Cell Behavior in the Polymeric Foams

#### 3.3.1. Distribution and Morphology of the Meningeal Cells on/in the Foams

The distribution and morphology of human meningeal cells on/in the foams were shown by their actin organization after Phalloidin-DAPI staining (Figure 4). It was seen that meningeal cells adhered and spread on

both foams produced with polymer solutions of 2.5% and 3% P(L-D,L)LA. Even the polymer preparation concentration did not change the cell behavior in terms of cell adherence and spreading, it seems that more cells were found on/in the foams of 3% P(L-D,L)LA compared to the foams of 2.5% P(L-D,L)LA. The high magnified images (Figure 4b and 4e) showed that cells spread along the pore surfaces of the foams. The analysis of cells with LSCM displayed that the cells were homogeneously distributed throughout the foam along z-direction (Figure 4c and 4f). The cells were not limited to the surface of the foams, they were also able to penetrate through the pores of the foam. *In vitro* studies revealed that the porosity and pore size of the developed dura substitute ensure uniform distribution of cells in 3D.

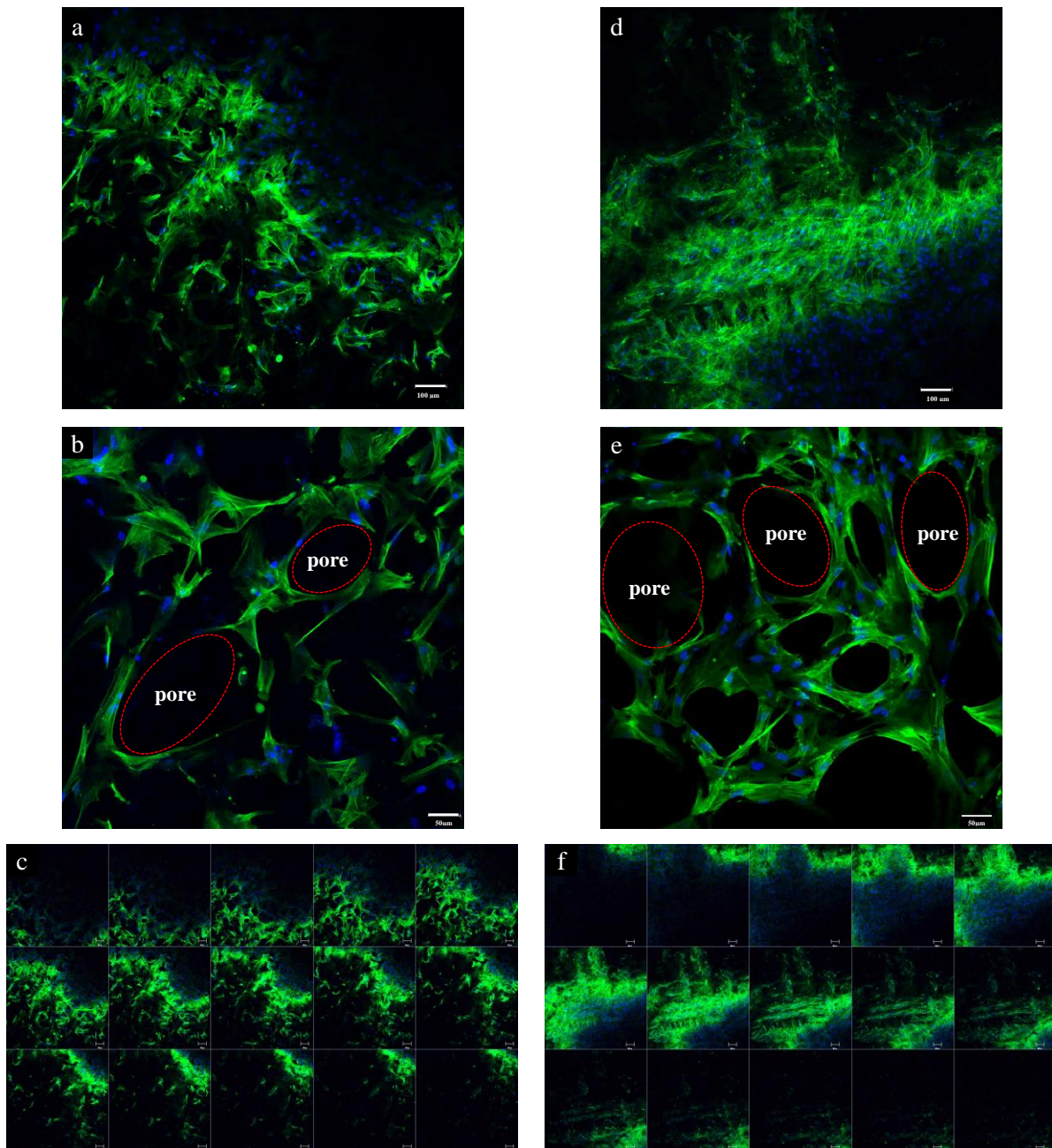


**Figure 4.** LSCM images of the human meningeal cells in the polymeric foams prepared with **a-c**) 2.5% and **d-f**) 3% P(L-D,L)LA solution. **c, f**) Images of optical sections through the samples in z-direction. The cells were stained with FITC-Phalloidin (green) for actin filaments and counterstained with DAPI (blue) for nucleus. Magnification, scale bar: **a, d, c, f**) 10X, 100 $\mu$ m, **b, e**) 20X, 50 $\mu$ m.



### 3.3.2. Proliferation of the Cells in the Foams

MTS assay results showed that meningeal cells exhibited similar growth profiles on both foams produced with polymer solutions of 2.5% and 3% P(L-D,L)LA (Figure 5). The results of Day 1 showed that the cells attached to both foams, and in fact, more cells were able to attach to the 3% P(L-D,L)LA foams. The number of cells on both foams increased significantly by at least 2-fold within 7 days, and this significant increase continued linearly, reaching 3- to 4-fold by Day 14. The rate of cell proliferation decreased after Day 14 in both foams, which could be due to cell-to-cell contact inhibition as the cell number increased. On Day 14, the cell number in the foam of 3% P(L-D,L)LA was significantly higher compared to the foam of 2.5% P(L-D,L)LA, confirming the Phalloidin-DAPI staining results.

In tissue engineering, it is suggested that a scaffold should have pores of sufficient size and quantity, typically ranging from 50 to 200  $\mu\text{m}$ , to facilitate cell infiltration and proliferation (Li et al., 2017). In this study, it was observed that the meningeal cells, fibroblast-like cells, penetrated into the foams, survived, grew, and spread in the foams with pore sizes ranging from 80 to 150  $\mu\text{m}$ . It was reported that the regeneration of dural defects is primarily driven by the development of connective tissue fibers and fibroblastic proliferation (Khurana et al., 2024). Consequently, these results suggest that the foams produced with 2.5% and especially 3% P(L-D,L)LA polymer solutions would serve as an appropriate dura substitute to provide cell ingrowth and tissue integration, and thus it would be a potential dura substitute to promote regeneration of the dura mater.

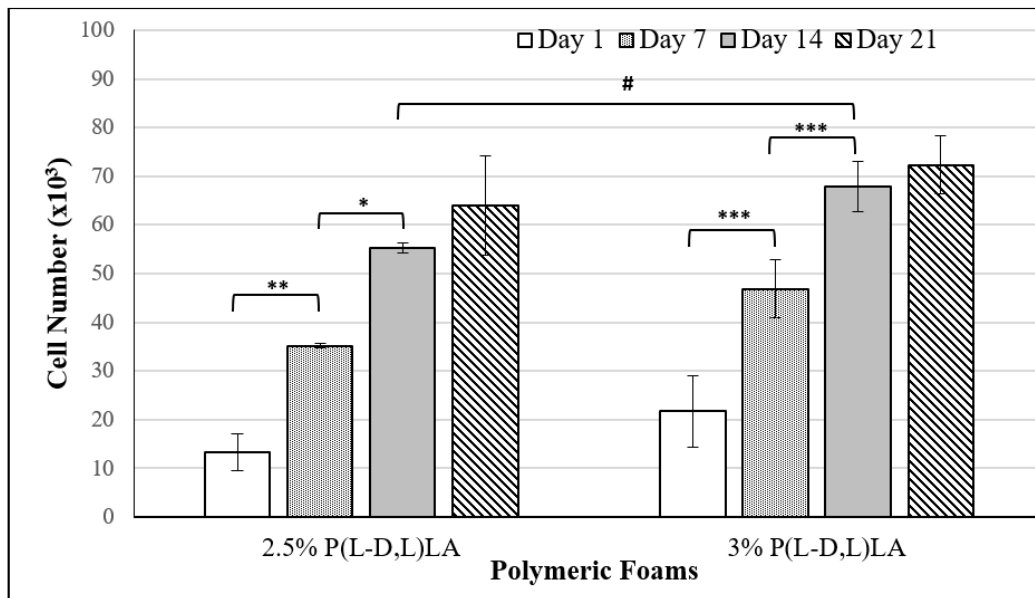


**Figure 5.** Proliferation of the human meningeal cells in the polymeric foams prepared with 2.5% and 3% P(L-D,L)LA solutions. The cell number in the foams at the 1<sup>st</sup>, 7<sup>th</sup>, 14<sup>th</sup> and 21<sup>st</sup> days of the culture. Statistical differences (# $p \leq 0.05$ , \* $p \leq 0.05$ , \*\* $p \leq 0.01$ , \*\*\* $p \leq 0.001$ ) are indicated.

## 4. CONCLUSION

Significant progress has been made in developing dural substitutes for repairing the dura mater. The studies in biomaterials and regenerative medicine aim to improve the performance and safety of these grafts, suggesting them as potential alternative treatments for future clinical applications. There are still some shortcomings with current dura substitutes, such as achieving ideal tissue compatibility and serving as a suitable scaffold to promote cell migration and tissue regeneration for structural and functional repair. The synthetic polymer P(L-D,L)LA (70:30) used in this study, as being GMP grade is appropriate to be used in medical device applications and could be suggested for the clinical studies after further *in vivo* performance analysis. Porosity is a critical factor for successful dural repair and regeneration, as it provides a favorable environment for cell integration and proliferation. In this study as well, it was found that the obtained foams with pore sizes in the range of 80 to 150  $\mu\text{m}$  allowed the spreading and growth of meningeal cells. This suggests that the dura substitutes

produced with 2.5% and especially 3% P(L-D,L)LA polymer solutions could provide a required, suitable environment for cell ingrowth and promote dura mater regeneration.

## ACKNOWLEDGEMENT

This study was supported by The Scientific and Technological Research Council of Turkey (TÜBİTAK) with the research project number SBAG 118S587. The author acknowledges the contributions of Acıbadem Mehmet Ali Aydınlar University (ACU) and Middle East Technical University (METU) Center of Excellence in Biomaterials and Tissue Engineering (BIOMATEN) for the use of the facilities and equipment, and METU Central Laboratory for mercury porosimetry analysis.

## CONFLICT OF INTEREST

The author declares no conflict of interest.

## REFERENCES

- Cho, M., Shim, K. M., Park, S. S., Kang, S. S., Jang, K., & Kim, S. E. (2024). Evaluation of Biocompatibility and Healing Properties of Dural Substitutes Produced by Electrospinning Technology. *In Vivo*, 38(3), 1119-1126. <https://doi.org/10.21873/invivo.13546>
- Choi, S.-W., Zhang, Y., & Xia, Y. (2010) Three-dimensional scaffolds for tissue engineering: the importance of uniformity in pore size and structure. *Langmuir*, 26(24), 19001-19006. <https://doi.org/10.1021/la104206h>
- Deng, K., Yang, Y., Ke, Y., Luo, C., Liu, M., Deng, Y., Tian, Q., Yuan, Y., Yuan, T., & Xu, T. (2017). A novel biomimetic composite substitute of PLLA/gelatin nanofiber membrane for dura repairing. *Neurological Research*, 39(9), 819-829. <https://doi.org/10.1080/01616412.2017.1348680>
- Deng, W., Tan, Y., Riaz Rajoka, M. S., Xue, Q., Zhao, L., & Wu, Y. (2021). A new type of bilayer dural substitute candidate made up of modified chitin and bacterial cellulose. *Carbohydrate Polymers*, 256, 117577. <http://www.doi.org/10.1016/j.carbpol.2020.117577>
- Dong, R.-P., Zhang, Q., Yang, L.-L., Cheng, X.-L., & Zhao, J.-W. (2023). Clinical management of dural defects: A review. *World Journal of Clinical Cases*, 11(13), 2903-2915. <http://www.doi.org/10.12998/wjcc.v11.i13.2903>
- Guimarães, A., Martins, A., Pinho, E. D., Faria, S., Reis, R. L., & Neves, N. M. (2010). Solving cell infiltration limitations of electrospun nanofiber meshes for tissue engineering applications. *Nanomedicine (Lond)*, 5(4), 539-554. <https://doi.org/10.2217/nmm.10.31>
- Kenar, H., Kose, G. T., & Hasirci, V. (2010). Design of a 3D aligned myocardial tissue construct from biodegradable polyesters. *Journal of Materials Science: Materials in Medicine*, 21(3), 989-997. <https://doi.org/10.1007/s10856-009-3917-8>
- Khurana, D., Suresh, A., Nayak, R., Shetty, M., Sarda, R. K., Knowles, J. C., Kim, H.-W., Singh, R. K., & Singh, B. N. (2024). Biosubstitutes for dural closure: Unveiling research, application, and future prospects of dura mater alternatives. *Journal of Tissue Engineering*, 15, 1-26. <http://www.doi.org/10.1177/20417314241228118>
- Klopp, L. S., Welch, W. C., Tai, J. W., Toth, J. M., Cornwall, G. B., & Turner, A. S. (2004). Use of polylactide resorbable film as a barrier to postoperative peridural adhesion in an ovine dorsal laminectomy model. *Neurosurgical Focus*, 16(3), 1-9. <http://www.doi.org/10.3171/foc.2004.16.3.3>
- Laun, A., Tonn, J. C., & Jerusalem, C. (1990). Comparative study of lyophilized human Dura mater and lyophilized bovine pericardium as dural substitutes in neurosurgery. *Acta Neurochirurgica (Wien)*, 107(1-2), 16-21. <http://www.doi.org/10.1007/BF01402607>
- Li, Q., Mu, L., Zhang, F., Sun, Y., Chen, Q., Xie, C., & Wang, H. (2017). A novel fish collagen scaffold as dural substitute. *Materials Science and Engineering C Materials for Biological Applications*, 80, 346-351. <http://www.doi.org/10.1016/j.msec.2017.05.102>

- Liao, J., Li, X., He, W., Guo, Q., & Fan, Y. (2021). A biomimetic triple-layered biocomposite with effective multifunction for dura repair. *Acta Biomaterialia*, 130, 248-267. <https://doi.org/10.1016/j.actbio.2021.06.003>
- Liu, W., Wang, X., Su, J., Jiang, Q., Wang, J., Xu, Y., Zheng, Y., Zhong, Z., & Lin, H. (2021). In vivo Evaluation of Fibrous Collagen Dura Substitutes. *Frontiers in Bioengineering and Biotechnology*, 9, 628129. <http://www.doi.org/10.3389/fbioe.2021.628129>
- Mai, R., Osidak, E., Mishina, E., Domogatsky, S., Andreev, A., Dergam, Y., & Popov, V. (2024). Collagen Membrane as Artificial Dura Substitute: A Comprehensive In Vivo Study of Efficiency and Substitution Compared to Durepair. *World Neurosurgery*, In Press. <https://doi.org/10.1016/j.wneu.2024.08.061>
- Mekhail, M., Almazan, G., & Tabrizian, M. (2012). Oligodendrocyte-protection and remyelination post-spinal cord injuries: a review. *Progress in Neurobiology*, 96(3), 322-239. <https://doi.org/10.1016/j.pneurobio.2012.01.008>
- Ohbayashi, N., Inagawa, T., Katoh, Y., Kumano, K., Nagasako, R., & Hada, H. (1994). Complication of silastic dural substitute 20 years after dural plasty. *Surgical Neurology*, 41(4), 338-341. [http://www.doi.org/10.1016/0090-3019\(94\)90187-2](http://www.doi.org/10.1016/0090-3019(94)90187-2)
- Patel, N., & Kirmi, O. (2009). Anatomy and imaging of the normal meninges. *Seminars in Ultrasound, CT and MR*, 30(6), 559-564. <http://www.doi.org/10.1053/j.sult.2009.08.006>
- Ramot, Y., Kronfeld, N., Steiner, M., Manassa, N. N., Bahar, A., & Nyska, A. (2024) Neural tissue tolerance to synthetic dural mater graft implantation in a rabbit durotomy model. *Journal of Toxicologic Pathology*, 37(2), 83-91. <https://doi.org/10.1293/tox.2023-0121>
- Rnjak-Kovacina, J., Wise, S. G., Li, Z., Maitz, P. K. M., Young, C. J., Wang, Y., & Weiss, A. S. (2011). Tailoring the porosity and pore size of electrospun synthetic human elastin scaffolds for dermal tissue engineering. *Biomaterials*, 32(28), 6729-6736. <http://www.doi.org/10.1016/j.biomaterials.2011.05.065>
- Schachtner, J., Frohbergh, M., Hickok, N., & Kurtz, S. (2019). Are Medical Grade Bioabsorbable Polymers a Viable Material for Fused Filament Fabrication? *Journal of Medical Devices*, 13(3), 0310081-310085. <http://www.doi.org/10.1115/1.4043841>
- Shi, Z., Xu, T., Yuan, Y., Deng, K., Liu, M., Ke, Y., Luo, C., Yuan, T., & Ayyad, A. (2016). A New Absorbable Synthetic Substitute With Biomimetic Design for Dural Tissue Repair. *Artificial Organs*, 40(4), 403-413. <http://www.doi.org/10.1111/aor.12568>
- Shijo, M., Honda, H., Koyama, S., Ishitsuka, K., Maeda, K., Kuroda, J., Tanii, M., Kitazono, T., & Iwaki, T. (2017). Dura mater graft-associated Creutzfeldt-Jakob disease with 30-year incubation period. *Neuropathology*, 37(3), 275-281. <http://www.doi.org/10.1111/neup.12359>
- Wang, M. O., Vorwald, C. E., Dreher, M. L., Mott, E. J., Cheng, M. H., Cinar, A., Mehdizadeh, H., Somo, S., Dean, D., Brey, E. M., & Fisher, J. P. (2015). Evaluating 3D-printed biomaterials as scaffolds for vascularized bone tissue engineering. *Advanced Materials*, 27(1), 138-144. <http://www.doi.org/10.1002/adma.201403943>
- Wang, W., & Ao, Q. (2019). Research and application progress on dural substitutes. *Journal of Neurorestoratology*, 7(4-5), 161-170. <http://www.doi.org/10.26599/JNR.2019.9040020>
- Wang, Y.-f., Guo, H.-f., & Ying, D.-j. (2013). Multilayer scaffold of electrospun PLA-PCL-collagen nanofibers as a dural substitute. *Journal of Biomedical Materials Research Part B Applied Biomaterials*, 101(8), 1359-1366. <http://www.doi.org/10.1002/jbm.b.32953>
- Welch, W. C., Cornwall, G. B., Toth, J. M., Turner, A. S., Thomas, K. A., Gerszten, P. C., & Nemoto, E. M. (2002). Use of polylactide resorbable film as an adhesion barrier. *Orthopedics*, 25(10), 1121-1130. <https://doi.org/10.3928/0147-7447-20021002-02>
- Yucel, D., Kose, G. T., & Hasirci, V. (2010). Tissue engineered, guided nerve tube consisting of aligned neural stem cells and astrocytes. *Biomacromolecules*, 11(12), 3584-3591. <https://doi.org/10.1021/bm1010323>